IEEE Access
Multidisciplinary ⋮ Rapid Review ⋮ Open Access Journal

Received August 3, 2019, accepted September 11, 2019, date of publication September 23, 2019, date of current version October 7, 2019.

Digital Object Identifier 10.1109/ACCESS.2019.2943120

Wireless Power Transfer With Magnetic Resonator Coupling and Sleep/Active Strategy for a Drone Charging Station in Smart Agriculture

AQEEL MAHMOOD JAWAD[1,2], HAIDER MAHMOOD JAWAD[1,2], ROSDIADEE NORDIN[1], SADIK KAMEL GHARGHAN[3], NOR FADZILAH ABDULLAH[1], AND MAHMOOD JAWAD ABU-ALSHAEER[4]

[1]Centre of Advanced Electronic and Communication Engineering, Faculty of Engineering and Built Environment, Universiti Kebangsaan Malaysia (UKM), Bangi 43600, Malaysia
[2]Department of Computer and Communication Engineering, Al-Rafidain University College, Baghdad 10064, Iraq
[3]Department of Medical Instrumentation Techniques Engineering, Electrical Engineering Technical College, Middle Technical University, Baghdad, Iraq
[4]Department of Statistics, Al-Rafidain University College, Baghdad 10064, Iraq

Corresponding author: Aqeel Mahmood Jawad (aqeel.jawad@ruc.edu.iq)

ABSTRACT Drones can be used in agriculture applications to monitor crop yield and climate conditions and to extend the communication range of wireless sensor networks in monitoring areas. However, monitoring the climate conditions in agriculture applications faces challenges and limitations, such as drone flight time, power consumption, and communication distance, which are addressed in this study. Wireless power transfer (WPT) can be used to charge drone batteries. WPT using a magnetic resonant coupling (MRC) technique was considered in this study because it allows high transfer power and efficiency with tens of centimeters, power transfers can be achieved in misalignment situations, charging several devices simultaneously, and unaffected by weather conditions. WPT was practically implemented based on a solar cell using a proposed flat spiral coil (FSC) in the transmitter circuit and multiturn coil (MTC) in a receiver circuit (drone) for the alignment and misalignment of two coils at different distances. FSC and MTC improved power transfer and efficiency to 20.46 W and 85.25%, respectively, at 0 cm with the loaded system under alignment condition. In addition, the two coils achieved appropriate transfer efficiencies and power for charging the drone battery under misaligned conditions. The maximum power transfer and efficiency were 17.1 W and 71% for the misalignment condition, at an air gap of 1 cm between two coils when the system was loaded with the drone battery. Moreover, the battery life of the drone was extended to 851 minutes based on the proposed sleep/active strategy relative to the traditional operation (i.e., 25.84 minutes). Consequently, a 96.9% battery power saving was achieved based on this strategy. Comparison results showed that the proposed system outperformed some present techniques in terms of the transfer power, transfer efficiency, and drone battery life. The proposed WPT technique developed in this study has been proven to solve the misalignment issue. Thus it offers a great opportunity as a key deployment component for the automation of farming practices toward the Internet of Farming applications.

INDEX TERMS Battery life, drone, energy efficiency, farming, flat spiral coil, flight time, multiturn coil, power consumption, wireless sensor network, solar panel.

I. INTRODUCTION

Drones can be used in the agriculture field [1]–[3] to monitor crop yield and climate conditions and to extend the communication range of monitoring areas. Drones can be equipped with several payloads, such as sensors, high-resolution and infrared cameras, tracking, and a global positioning system (GPS), as a delivery vehicle [4]. These drones generally run on batteries powered with high energy, such as lithium batteries, to enable flight times of

The associate editor coordinating the review of this manuscript and approving it for publication was el-Hadi M. Aggoune.

approximately 20–40 min [5], [6]. However, the battery lifetime is a problem faced by drone systems, particularly in cases where a stand-alone maneuver of the drone is required. Moreover, the battery charging problem of the drone has not yet been widely addressed and has the possibility for an intensive investigation [7].

Three ways can be adopted to improve drone flying time:

(i) Drones can be provided with high battery capacity. However, this solution increases drone weight, thereby is still not solving the operation time problem in addition to reducing the allocation for the other payload.
(ii) The battery can be automatically swapped after the drone lands at the base station [8]. However, this method is unfeasible because of the high cost and complexity of the swapping system, where an additional mechanical component is required.
(iii) The battery can be charged at the base station of the drone.

For the above solutions, two techniques can be implemented for the drone charging station. The first method is to use electrical contact between the drone and the base station [9]. The second method uses wireless power transfer (WPT) [10]–[13] or solar energy [14]–[20]. The former is considered in this study because the focus is on multirotor drones. Solar energy is suitable for fixed wing drones but displays several limitations for rotary wing drones, such as the requirement of a certain space that exists at the drone to be mounted; practically, rotary wing drones offer limited chances for implementing this type of energy. In addition, solar cells mainly depend on solar radiation, which is not always available and depends on the seasonal/temporal variation [7].

The electrical contact method is characterized by high efficiency. However, environmental conditions, such as temperature and humidity, reduce system reliability and efficiency. First, most WPT techniques allow for reliable and efficient power transfer between the base station and the drone. When the WPT method is applied to the drone, some critical issues, such as the payload and interference of the WPT system with communications between the drone and the base station, must be considered. The WPT system mounted on the drone should be lightweight to prevent payload reduction. In addition, the WPT technique should ensure high transfer power efficiency and misalignment tolerance between the transmitter and receiver coils of the WPT system. Misalignment is the dominant case in WPT specific for a drone application because often in this case, the landing accuracy of a drone is found to be very low. Consequently, the transfer coupling factor, transfer power, and to some extent the transfer efficiency decreases as described in [21]. Several articles have discussed the major concerns about recharging drone batteries via WPT [12], [22]–[26], and they are highlighted in the next section.

In this study, an X525 drone model was used to determine climate conditions, such as soil pH, air temperature, and humidity, and soil moisture from the farm field. The drone works as a router node in the proposed ZigBee WSN to transfer the data from the agriculture sensor nodes to the coordinator node. The router node mounted on the drone can be supplied by energy using a 1 W/5 V solar cell. WPT is used to charge the drone battery to improve its lifetime. A substantial enhancement in the coil design of the proposed WPT system is observed by considering the misalignment between the transmitter and the receiver coils. The suggested solution includes the design of a high-efficiency charging or transmitter coil (fixed on the platform) or a flat spiral coil (FSC) that is approximately 150 coil turns with 40 cm coil diameter and 1.02 mm (18 AWG) wire thickness. The secondary or receiver coil mounted on the drone, i.e., multiturn coil (MTC) that is 60 coil turns with 40 cm diameter and 0.51 mm (AWG 24) wire thickness. To this end, a drone is charged based on a new WPT system design. The WPT system is designed, implemented, tested, and installed on the manufactured X525 drone by keeping good performance metrics, such as transfer power, transfer efficiency, transfer distance, suitable payload, and maintaining drone maneuvering. In addition, the misalignment between the transmitter and receiver coils is investigated.

The main contributions of this study can be summarized as follows:

(i) This work is an extension to the previous study in [27]. The previous work was limited to low-power-consumption home devices such as shavers, smartphones, and toothbrushes. As such, the circuit developed from the past works was found to be inapplicable for high-power electronic applications. In this work, we extended the circuit to charge the medium-power electronic devices such as a drone for potential deployment in future smart farm applications.
(ii) We improved the power transfer and efficiency by solving the misalignment condition between the transmitter and receiver coil. The previous work in [27] did not address the misalignment problem. The improvement came from a novel design and hardware development of the FSC in the transmitter circuit and the MTC in a receiver circuit that is located at the drone charging station.
(iii) The power consumption and battery life of the drone-based agriculture application were formulated and modeled. This involved measurement from the magnetic resonator coupling WPT prototype that charges the drone's battery when the drone is on the landing position in the charging station after each agriculture mission.
(iv) A sleep/wake strategy is proposed to increase the energy saving further from the wireless sensors network. Performance comparisons are made with other techniques in previous studies, in terms of transfer power and transfer efficiency under the alignment scenario.

II. RELATED WORKS

Wireless power charging has been recently investigated in several research works. Campi *et al.* [22] proved the feasibility of the magnetic resonant coupling (MRC)/WPT charging system applied to a demonstrative drone that could be used in various applications. Different misalignment topologies and distances were tested. The transfer efficiency of 90% was achieved at 10 cm to charge the drone. Campi *et al.* [13] proposed a high-power and high-efficiency WPT system based on MRC and automatically recharged the battery of a small unmanned aerial vehicle (UAV). A total flight time of 20–60 min and transfer efficiency of 93% was achieved at 10 cm. An 85% transfer efficiency was accomplished with a misalignment transfer distance of 8 cm. Moreover, Campi *et al.* [28] tested different misalignments in two dimensions (x-axis and y-axis). The proposed design achieved 85%, 81%, and 76% at 0, 10, and 20 cm, respectively. The main advantages of all onboard components are as follows: lightweight and compact to minimize size and weight as much as possible. An operating frequency of 150 kHz was adopted for the design of the three studies.

Zhou *et al.* [29] proposed a novel nonlinear parity-time-symmetric model to inspect a transmission line tower. The WPT system was investigated for different alignments at distances of 2, 4, 6, 8, 10, 12, 14, and 16 cm at 10 W load power and 1 MHz operating frequency. Experimental results show that when the flying drone hovers in a confined 3-D volume of space above the WPT platform, the stable output power is maintained with an approximately constant transfer efficiency of 93.6%. In particular, for the experimental prototype, the output power and transfer efficiency can remain nearly unchanged within the lateral misalignment range between 0 and 6.5 cm for the transfer distance equal to 8 cm. However, a transfer efficiency of 50% can be obtained when the coupling region is weak.

Aldhaher *et al.* [10] presented an overview of the technologies that enabled ultra-lightweight WPT systems, which were tolerant of changes in the air-gap geometry. They enable drone charging in mid-air, thereby enabling 7 min flying time. The WPT system operates at a high frequency of 13.56 MHz with a charging capacity of 10 W while hovering the drone. Drone charging can be achieved within the vicinity of a pad at a distance of 12 cm. Griffin and Detweiler [30] developed an MRC power transfer system that enabled a UAV to provide power to the batteries of wireless sensors and other electronics that were removed far from the electric grid. Their experiments verified a WPT system that enables a UAV to power and recharges ground sensors. Two types of techniques are used, namely, (i) developing an MRC power transfer system and (ii) the use of the AscTec Hummingbird quadrotor helicopter. The first technique has an adequate quality factor, whereas the second one carries the transmitting coils and power system. The quadrotor has a flight time of 15–20 min when using a 2.1 Ah, 11.1 V lithium polymer (Li-Po) battery. The MRC system works between 190 and 210 kHz. The battery can provide more than 550 W. However, the UAV loses as much as one-third of its flight time when providing power transfer. The experimental results show that the UAV transmission does not accomplish as much power transfer as the static case in large part due to the relative motion and deformations of the drive and Tx coils on the helicopter.

Wang and Ma [31] developed an MRC power transfer system that allowed a UAV to supply low power to solve the problem of UAV endurance. The authors designed a UAV that can cruise automatically, self-charge, and transfer data by using an autonomous cruise network system that consists of a plurality of intelligent charging rods and GPS devices. The main problem of the UAV is that it cannot perform remote tasks because of its weak cruising ability. They proposed a charging station with two solar cells to solve this limitation of the battery and range of any flying device, such as drones. Battery capacity is mostly between 5 and 16 Ah. UAV battery capacity must be considered in the selection of a battery. Therefore, they used solar batteries for models 65, 80, 100, 150, and 200 Ah. The use of 12 V 100 Ah batteries is recommended to ensure the endurance of UAVs, by analysis and calculation considering the possible impact of weather and other reasons for solar panels to generate electricity. This type of battery can provide a UAV (22.2 V, 16 Ah) with 3–4 full charging times. The normal 22.2 V 7 Ah of a UAV can be fully charged 7–8 times, thereby meeting the basic requirements. At the same time, solar panels can fully charge the battery in two and a half days by selecting 100 W solar panels as energy storage battery supplement under normal weather conditions. The results show that the transfer efficiency of 90% was obtained at a distance of 5 cm with a high transmission power of 130 W, which adequately meets the requirements of UAV wireless charging via WPT.

Junaid *et al.* [11] proposed a vision-based, closed-loop target detection using a UAV in outdoor environments. A wireless charging station that allows autonomous landing and charging of a UAV without any human intervention was developed to enhance endurance and prolong the flight time of the UAV. Analysis and experimental results revealed good performance, and 10 W of transfer power and 75% efficiency were accomplished. The flight time of approximately 12 min was achieved based on the full charging cycle that lasts approximately 1 hour based on the proposed WPT.

Valente *et al.* [3] proposed a solution based on the combination of UAV and WSN to monitor variables from fragmented crop fields. They presented a collaborative system made up of a WSN and an aerial robot, which is applied to real-time frost monitoring in vineyards. The proposed system ensured communication (based on XBee wireless technology) between the base station and the sparse clusters placed at split parcels. In their experiments, they adopted a small quadrotor with 200 g payload, 550 g whole weight, and 2100 mAh/11.1 V Li-Po battery capacity and whose weight of control and communication components is less than 50% of the payload capacity. Through the experiments, a maximum drone speed of 5 m/s was able to fly with a battery along 5000 m.

They provided many advantages to consider ground WSN, such as the development of the WSN communication workflow, development of the data routing to the base station, and better monitoring of the crop. However, the power consumption was not analyzed in this study.

Faiçal *et al.* [1] described an architecture to address the problem of self-adjustment of the UAV routes when spraying chemicals in a crop field. They presented an algorithm to adjust the UAV route to wind changes (intensity and direction) and the impact caused by the number of messages exchanged between the UAV and the WSN. Twenty-two sensor nodes were distributed in the crop field of 1000×50 m^2. The UAV speed and operating heights are 15 m/s and 20 m, respectively. Light and moderate winds are described to have a speed of 10 km/h and 20 km/h, respectively. The results show that the communication time between a sensor ground (XBee-PRO S2) and the UAV was between 0.035 and 0.042 s for different UAV heights of 5, 10, and 20 m. As a result, the communication time between the UAV and the WSN when the XBee-PRO S2 was employed showed no substantial difference for the adopted heights.

Polo *et al.* [32] proposed an agricultural environment monitoring server system that used a low-cost WSN, and the fixed wing UAV might be utilized to cover the long communication distance. The UAV must cover distances of up to 10 km or to operate in fields of approximately 100 ha. They used a Turing Nano-tech 8400 mAh/11.1 V battery. This battery provides approximately 25 min of autonomous operation, and the range is approximately 27 km. One of the initial design requirements requires the total weight of the system, including the main aircraft, to be 5 kg. The maximum payload contained in the tank is 2 kg because the total weight of the airplane is 3 kg. The results show that when the mobile node collects the data stored in a ground node, it needs 129 ms to retrieve the data recorded in 1 day. The usual speed and flight altitude of the drone (mobile node) are 18 m/s and 20 m, respectively. In this condition, the mobile node needs to consume 10.9 s to collect the data from a ground node within 100 m. This time is adequate for covering 1814 measurement samples, which is symmetrical to approximately 12.5 days of measurements. This measurement is enough to ensure the transfer of agricultural field information from the sensor network to the mobile node.

Mittleider *et al.* [33] presented a novel method for charging WSNs based on UAVs. UAVs can be accurately localized to 15 cm based on magnetic resonant sensors wherein the GPS is inaccurate and needs line-of-sight between the receiver and the satellite. However, the charging efficiency can be increased when the transmitting (mounted by a UAV) and receiving (fixed in the sensor node) coils are close to each other. Consequently, the charging power of 5.49 W for a 6 cm distance between the receiving and transmitting coils is adequate for charging the battery of wireless sensor nodes at a remote location.

Blain [21] presented a new mid-air inductive charging technique that was able to charge several drones at the same time without needing them to land utilizing suggested global energy transmission (GET). The GET consists of a hexagonal structure of energy lines fixed on poles approximately 10 m in diameter. However, when a correctly set up drone hovers into it, the GET can transfer up to 12 kW of power at efficiencies of 80%. Thus, the drone can fly about 25 minutes and 6 minutes stop in the air for battery charging. Consequently, the drone can stay in the air for a long time and never needs to land. However, this technique requires high energy resources to transfer such high power into the air.

III. WPT SYSTEM DESIGN

The following subsections describe the mathematical analysis of the WPT, the adopted coils designed with related parameters, the WPT system designed for alignment and misalignment, and experiments with load for the aligned and misaligned coils.

A. WPT MATHEMATICAL MODEL

Varying dynamic wireless environments show a dynamic coupling factor (K). The coils are made from copper wires to reduce the alternating current (AC) losses due to skin and proximity effects. The coupling factor K is given by [34].

$$K = M/\sqrt{L_r L_s} \tag{1}$$

A coupling coefficient K is generally used to indicate the amount of coupling between two coils, as shown in Equation (1), where M is the mutual inductance between the two coils, and L_r and L_s are the self-inductances of the transmitting and receiving coils, respectively. A high value of K(up to a maximum of 1) indicates that a large portion of the magnetic field generated by the transmitter coil is coupled into the receiving coil, wherein K increases as the coils approach each other. In loosely coupled WPT systems, the values of K are extremely low. The two primary factors for resonant coil performance are that they resonate close to the same frequency and they have a sufficiently high quality factor. The quality factor represents how well a resonant coil can hold energy without losses to heat. For determining the resonant frequency of a coil, its inductance must be calculated first [7].

$$L = \mu_o r N^2 \left(ln\frac{8r}{a_i} - 1.75 \right), \tag{2}$$

where L is the inductance of the coil (mH), μ_o is the vacuum permeability which equals $4\ \pi \times\ 10^{-7}$ H/m, r is the loop radius of the coil, N is the number of coil turns, and a_i is the radius of the wire cross section.

The resonant frequency (f_o) for the input and the output in Equation (3) can then be computed, given capacitance (C) and inductance (L), with the following equation [35]:

$$f_o = \frac{1}{2\pi\sqrt{LC}} \tag{3}$$

The other component is the quality factor of the resonant coils (Q_R), which can be found from [36] with the

following equation:

$$Q_R = \frac{1}{R}\sqrt{\frac{L}{C}}, \tag{4}$$

where R is the resistance of the coil (Ω). The quality factor can be increased in two ways to lower capacitance or resistance, as shown in Equation (4). Capacitance is easily decreased by either pairing a capacitor in series or by using new capacitors with a low value. The real effect of a low capacitance is a high resonant frequency, as shown in Equation (3), which limits significant currents from voltages having less time to overcome magnetic momentum. The other method for raising the quality factor and lowering resistance is achieved by using a low gauge wire for the resonant coils. However, low gauge wires are heavy, and the amount of weight a UAV can carry is limited.

Finally, the transfer efficiency η_T can be calculated based on Equation (5) by dividing the DC output power (P_{DC_output}) by the DC input power (P_{DC_input}) [37].

$$\eta_T = \frac{P_{DC\_output}}{P_{DC\_input}} \tag{5}$$

B. WPT COIL DESIGN

The design process of the transmitter coil can be described as follows. A square wooden pad was used as a base to wind the coil. The wooden pad size was 50 × 50 cm^2, and its thickness of 1.5 cm was selected to avoid the deformation of the base during the winding. A 2 mm hole was drilled in the center of the wood pad to insert one end of the wire. 18 AWG (1.02 mm) copper wire was adopted in the transmitter coil. Next, the process of winding of the coil was started until 150 turns were completed as shown in Figure 1(a), which is also equivalent to 40 cm coil diameter. We applied super glue between turns to maintain the shape of the coil.

The receiver coils were also mounted on the wooden pad for the same reason. A circle with 40 cm diameter was drawn to be identical with the diameter of the transmitter coil. Then, several screws were fixed on the circumference of the circle to give a circular shape as shown in Figure 1(b). The circular shape is used in this study because a circular shape gives more enclosed space (area) for a given distance (perimeter/circumference) than a square does, which results in higher transfer efficiency. Next, the process of winding of the coil (Figure 1) is started until the required turns were achieved. When the winding of the coil was finished, the coil was tied using cable ties. Copper wire with 24 AWG (0.51 mm) was used to design several coils with 50, 60, 100, and 150 turns. In addition, 18 AWG (1.02 mm) was considered to design coils with 25, 75, and 100 turns. Various copper coil sizes are considered in this study to select the ideal coil that can achieve high transfer power and efficiency while keeping suitable coil weight.

Several coils with two AWG were designed to select the best coils for the transmitter and the receiver that can achieve maximum power transfer, as shown in Figure 1. Consequently, coil a (Figure 1(c)) was selected for the transmitter and b (Figure 1(d)) was designated for the receiver. Coil a was designed as an FSC to ensure the alignment with the receiver coil and to transfer maximum power. The coil was made by using copper wire with 150 turns, a coil diameter of 40 cm, and a thickness or wire diameter of 1.02 mm. In this case, the measured inductance was 0.29317 mH to generate a resonant frequency of 12 kHz when it is connected to a 0.6 μF parallel capacitor based on Equation (3). The low oscillating frequency (i.e., 12 kHz) was selected in this study due to (i) the zero-voltage switching (ZVS) oscillator available in our lab is limited to this frequency, where the transmitter coil is permanently on the charging station (ii) low frequency reduces parasitic losses, whereas it is dominant in high frequency [38], and (iii) higher frequency is suitable for using with a series resonator circuit [39], therefore it does not used in the current application since the adopted of the ZVS limited to parallel resonator. The available ZVS oscillator is not compatible with the lightweight coil and the small number of turns due to large heat dissipation. Due to this limitation, we considered heavy weight coil and the large number of turns in the current work. The novelty of our work lies on several improvements, which include payload capacity, flight time, transfer power, transfer efficiency, development of sleep/wake algorithm, as well as solving the drone misalignment issue. The receiver coils were designed as MTCs implemented with a large diameter of 40 cm. One of the coils was installed on the end of the drone's hand grips away from the control and communication parts to avoid electromagnetic interference between the coils and the components [28]. The specifications of the adopted coils were measured and are presented in the next section (Table 1).

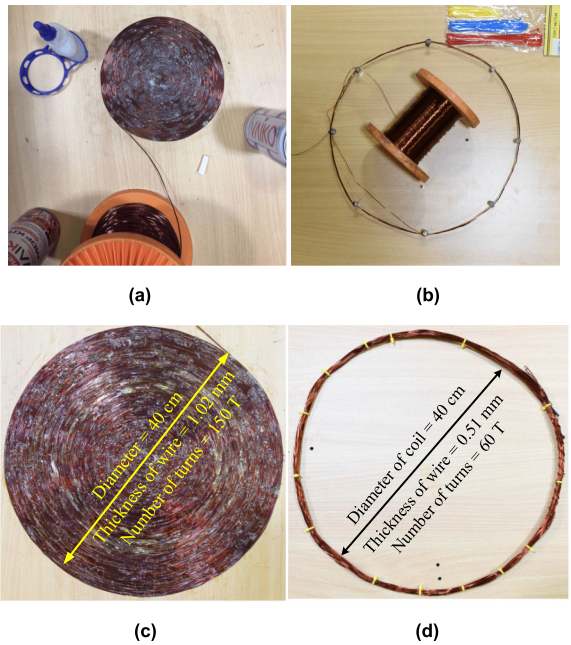

FIGURE 1. The designed coils: (a) design process of the transmitter coil, (b) design process of the receiver coil, (c) transmitter coil, and (d) second coil: receiver coil for the second design.

TABLE 1. Specifications and parameters of transmitter and receiver coils.

Specification of coils	Transmitter coil (c)	Receiver coil (d)
Number of turns	150 T	60 T
Thickness of wire (mm)	1.02	0.51
Inductance (mH)	0.29317	4.039
Quality factor (Q)	24.33	13.69
Weight (g)	720	290
Resistance of inductor (Ω)	1.3427	4.323
Diameter of coil (cm)	40	
Air gap between (cm)	0–100	
Operating frequency (kHz)	12	
Operating source	24 V/1 A	

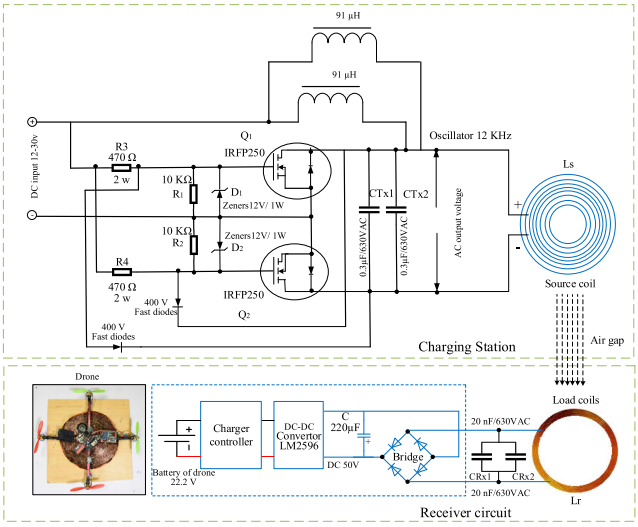

FIGURE 2. Schematic of the implemented WPT system.

C. WPT SYSTEM DESIGN

The main objective in designing a WPT system is to recharge the battery of the drone. In the implemented WPT system, the transmitter coil is properly chosen from the FSC placed on the pad of the base station, while the receiver MTC is selected based on several tested coils. We selected the coil that can transfer the maximum power while maintaining the weight of the drone payload as much as possible. The receiver coil is placed on the end of the drone's hand grips to reduce the vertical distance between the receiving and transmitting coil. This solution allows for a considerable improvement in system performance by an increase in the coupling coefficient between the coils. A parallel to parallel (P–P) compensation [27] is selected in the transmitter and the receiver circuits, as shown in Figure 2. The receiver coil is used to charge the battery of the drone. This study considers a 22.2 V/5500 mAh Li-Po battery for the X525 quadcopter drone.

The source or transmitting circuit comprises an FSC and an oscillator circuit (i.e., ZVS 1000 W/20 A with a DC input voltage of 12–30 V), which generates a frequency of 12 kHz. This circuit generates oscillations using two metal-oxide-semiconductor field-effect transistors (IRFP250N), two general-purpose Zener diodes (12 V/1 W), two fast diodes,

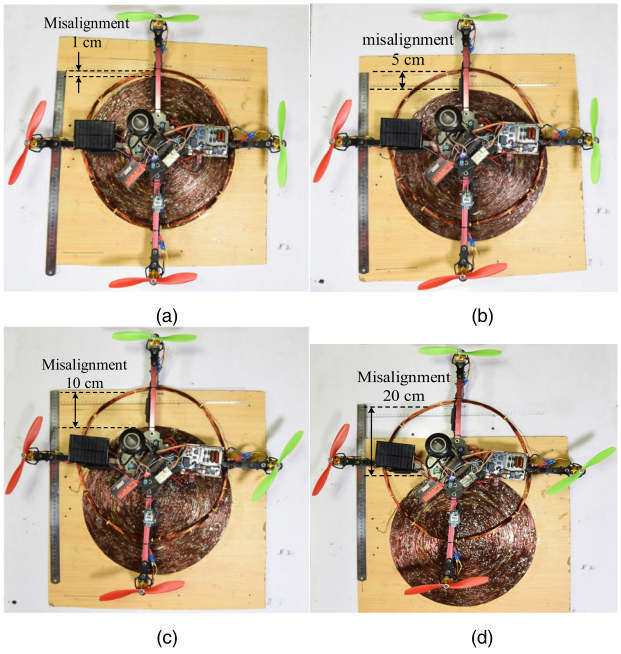

FIGURE 3. Misalignment test: (a) 1 cm, (b) 5 cm, (c) 10 cm, and (d) 20 cm.

two parallel coupling capacitors, two radio-frequency choke coils, and four resistors. The main components of the receiver circuit consist of the MTC, two parallel coupling capacitors, a bridge rectifier, an LM2596 DC–DC converter (Texas Instruments, Dallas, TX, USA), and a charging controller to charge the battery of the drone with a suitable voltage (i.e., 24 V). Here, the battery of the drone can be used as a load for the receiver circuit. The specifications and parameters of the transmitter and receiver coils of the WPT system are shown in Table 1.

D. MISALIGNMENT CONFIGURATION

In this study, the high level of possibility for solving the lateral misalignment condition is achieved by adopting a large primary and secondary coil configuration, as illustrated in Figure 3. The second design, which is presented in Figure 1(d) (i.e., MTC with 60 turns) is employed in the receiver circuit for the lateral misalignment test with the transmitter coil. The pad of the base station is implemented to ensure a lateral misalignment of not more than 20 cm between the transmitter and the receiver coils. However, four different misalignment distances of 1, 5, 10, and 20 cm were experimentally tested to evaluate the energy transfer performance, as shown in Figure 3(a), (b), (c), and (d), respectively. The transfer power and efficiency are measured for these distances for the drone landing. The transferred energy is investigated for different distances between 0 and 24 cm for each lateral misalignment. The direct current (DC) and voltage are measured every 1 cm, and the DC output power and transfer efficiency are calculated when the receiving circuit is loaded by the battery of the drone.

TABLE 2. Summary and difference between experiment setup.

Experiment	Scenario	With Load	No. of coils	No. of turns	Misalignment Distance (cm)
First	Alignment	Yes	1	60	No
Second	Misalignment	Yes	1	60	1, 5, 10, and 20

E. WPT EXPERIMENT CONFIGURATION

The WPT system is intended for charging low-power-consumption devices, such as low electronic appliances [27] and drones. However, the proposed FSC (transmitter) and MTC (receiver) topology generate strong leakage magnetic fields. The measurement of the proposed MTC WPT at different distances is shown in Figure 4(a) (alignment system) and 4 (b) (misalignment system). Two designs are implemented and experimentally tested as follows and summarized in Table 2. The first and second experiments were conducted in the presence of a load. Once the best coil has been identified, it is later used in the first and second experiments under the load conditions.

(i) **First Experiment** The experiment is implemented for an alignment system with a load. The FSC is tested with the second coil, which was previously shown in Figure 1(d). The second coil consists of one tap (i.e., 60 turns). The number of turns is selected based on the first and second experiments, wherein a tradeoff between coil weight, transfer power, and efficiency is achieved to obtain acceptable transfer performance and weight.

(ii) **Second Experiment** The experiment is implemented for a misalignment system with a load. A total of four lateral misalignment distances (1, 5, 10, and 20 cm) are investigated in this experiment. The FSC is tested with the second coil (i.e., 60 turns), which was previously shown in Figure 1(d).

The FSC is constant in all the experiments, whereas the MTC is moving with constant air-gap steps. In the first and second experiments, air-gap steps of 5 cm until 100 cm are adopted. For the first and second experiments, air-gap steps of 1 cm until 24 cm are considered. The difference in the air-gap steps for the experiments is attributed to the proposed loaded and unloaded WPT system, wherein the transfer power and efficiency are decreased to a large extent after 24 cm in the loaded system. For each position, the transfer voltage, current, power, and efficiency are measured with respect to the distance, as presented in the results section. The measurements are conducted in a laboratory, as shown in Figure 4(a) and 4(b), using a digital multimeter (DT9205, Dowdon), an oscilloscope (MCP Lab Electronics/DQ7042C, Shanghai MCP Corp.), and a measurement tape (0–100 cm). In addition, a DC power source (GPS-3030D, Cole-Parmer) is employed to supply the transmitter circuit.

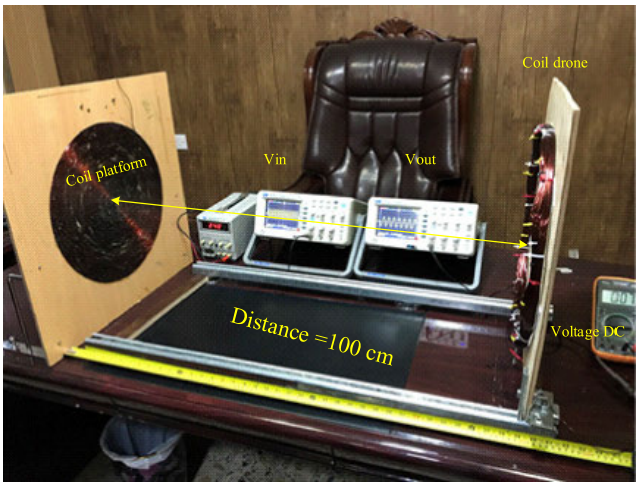

(a)

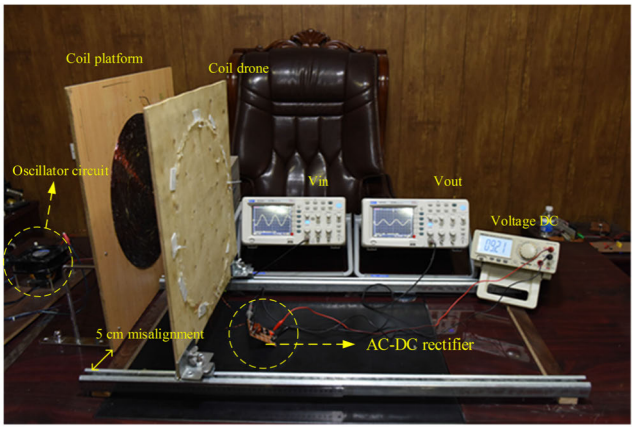

(b)

FIGURE 4. Measurement of the implemented WPT at different distances in the laboratory for (a) alignment system and (b) misalignmen system.

IV. DRONE SYSTEM DESIGN

The following subsections highlight the flight time and power consumption analysis, the design and implementation of the drone with related components, and the platform charging with the structure.

A. FLIGHT TIME AND POWER CONSUMPTION ANALYSIS

The drone flight time F_t, which is expressed in hours, can be calculated mainly based on the battery capacity C_b, which is expressed in amp-hours (Ah). A 5.5 Ah system is considered in our study and the active drain current of the drone (A_d) is measured in A. The drone flight time can be governed by a single formula as follows:

$$F_t = C_b \times D_b / A_d, \tag{6}$$

where the D_b is the battery discharge allowed during the flight. It is common to not discharge Li-Po batteries by more than 80% in experiments because they may be damaged if fully discharged.

The average drain current of the drone (A_d) can be computed by applying Equation (7).

$$A_d = W_T \times P/V, \tag{7}$$

where W_T is the total weight of the drone that goes up in the air, including the MTC of the WPT and all the installed components, measured in kg. In our application, the total weight is approximately 1.892 kg, P is the lifting power of 1 kg of the apparatus expressed in W/kg, which is approximately 120 W/kg, and V is the adopted battery voltage, which is 22.2 V in this experiment.

The drone battery lifetime B_{LT} in a traditional operation can be computed based on Equation (8).

$$B_{LT} = (C_b/A_d) \times (1 - D_s), \tag{8}$$

where D_S is the battery discharge safety which indicates the fraction of the battery that is never used. The adopted Li-Po battery is not discharged below 20% to avoid damage.

We further applied a sleep/wake strategy to improve the drone battery lifetime. The drone can enter sleep mode when it is not on a mission in the farm field. This task can be achieved automatically when the drone lands on the pad of the base station by switching off the battery from the drone using a small controller circuit. The controller circuit is switching between ON and OFF. When the drone is on the landing position, the controller disconnects the drone from the battery and connects it to the charging circuit. Thus, the power of the battery can be saved. In this case, the formula for the drone average current consumption, A_{avg} can be expressed as

$$A_{avg} = [(A_d \times T_1) + (A_s \times T_2)] \big/ (T_1 + T_2), \tag{9}$$

where A_s is the current consumption in sleep mode, and T_1 and T_2 are the active and sleep times, respectively.

The battery power saving of the drone can be calculated as Equation (10),

$$Power\ savings\,(\%) = (A_d - A_{avg}) \big/ A_d, \tag{10}$$

B. DRONE COMPONENT INSTALLATION

The components and the apparatus should be distributed throughout the drone's body. The first limitation of the WPT design is that the size, weight, and shape of the receiver coil (i.e., MTC) must be effectively designed to recognize the apparatus. Meanwhile, the charging system-based WPT system should be sensibly efficient in terms of transfer power and efficiency.

The drone (X525 quadcopter) is assembled and equipped with a 60-turn MTC wireless charging coil to charge its battery. The receiving coil is placed on the end of the drone's hand grips with no air gaps (i.e., 0 cm) between the FSC of the transmitter circuit and the MTC of the receiver circuit, as shown in Figure 5. The payload of the drone poses a challenge in our MTC design. Consequently, the weight of the MTC is reduced as much as possible to 290 g, and the final total weight of the drone is 1.892 kg. The drone for this research is able to carry 0.555 kg payload. Based on the circuit and electronic components attached to the drone, it can be observed that the WPT circuit and components only take 41.51%, i.e., (0.555/1.337) × 100% of the payload. The weights for the different parts of the drone are shown in Table 3. For1000 V/4 A diodes are used as the AC to DC rectifier circuit. The 55 V DC output (with no air gap between the MTC and the FSC) is converted to 24 V to charge the battery of the drone based on the step-down LM2596 DC–DC converter, and then the output is connected to a charge controller to control the charging process of the battery of the drone.

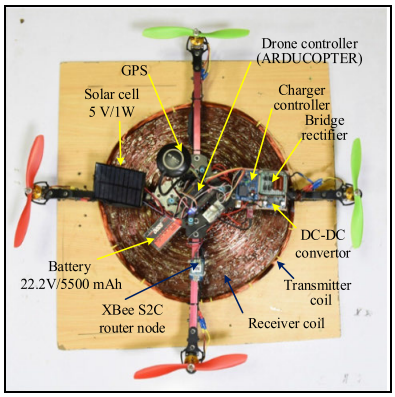

FIGURE 5. X525 quadcopter drone landing support.

TABLE 3. Calculation of drone weight.

Parameter	Weight (kg)
ZigBee (S2C) with Base	0.009
Base of Receiver Charging	0.105
Solar cell (1 W/5 V)	0.019
Base of Battery with Charge Controller (5 V)	0.045
Two Battery Li-Ion (7.4 V/2600 mAh)	0.087
Secondary Coil	0.29
Payload weight	0.555
Drone weight	1.337
Ratio of payload weight to the drone weight	41.51%
Ratio of on-board coil weight to the total drone weight	21.69%

The charging controller disconnects the charging current and voltage from the battery when it becomes fully saturated. These elements are mounted on a board on the top side of the drone's body, as shown in Figure 5. In addition, the drone includes a ZigBee S2C router node, a 1 W/5 V solar cell to supply energy to the router node, a drone controller (ARDUCOPTER), a GPS, and a 22.2 V/5500 mAh Li-Po battery. The router node, which is supplied with power by the battery and the 1 W/5 V solar cell, can enter sleep mode to save energy when there is no data transmission.

C. DRONE CHARGING PLATFORM DESIGN

The drone base station is shown in Figure 6. It is manufactured to meet the requirements of the drone and the farm fields in terms of power sources and structure. The frame of the base

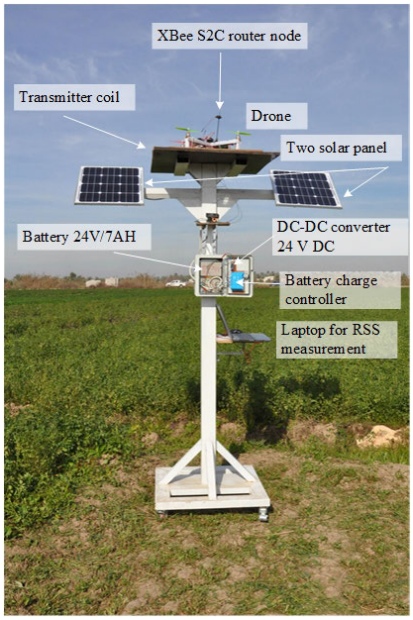

FIGURE 6. The base station of the drone.

station is made from steel. The height of the station is 2.7 m from the ground. The base station consists of:

(i) A 50 cm × 50 cm FSC WPT pad for landing and takeoff
(ii) An FSC WPT coil with a 1 A/12–30 V DC input ZVS oscillator circuit
(iii) Two 2 × 30 W 60 W/36 V solar panels positioned on the left and right sides of the station frame with an inclination of 30° to face the sun
(iv) A rechargeable 24 V/7 Ah battery
(v) An LM2596 DC–DC converter
(vi) A battery charger controller, and
(vii) A force-sensitive resistor (FSR) to switch the drone charging on and off.

When the drone lands on the station, the FSR sensor senses the weight of the drone and turns on the charging circuit. Otherwise, the FSR sensor turns off the charging circuit to keep the ZVS oscillator circuit and the FSC in the off state during a drone mission in the farm field and to save the energy of the base station's battery.

The solar panels are used to charge the base station battery through the DC–DC converter and charger controller. The battery supplies the ZVS oscillator circuit and the FSC with DC power during the drone's landing. The solar panels are sufficient for fully charging the battery of the base station with the required charging voltage (i.e., 24 V) and current (1.667 A) in less than 4.8 h. This charging period is shorter than the mission cycle of the drone, wherein one mission cycle is planned every six hours to collect the data of the sensor nodes distributed in the farm field. Thus, the battery of the base station can be safely recharged.

V. EXPERIMENTAL RESULTS AND DISCUSSION

Two experiments were conducted based on the number of coils turns to select the best one for the drone in terms of transfer power and efficiency and to ensure the lightweight payload of the drone. The results from several test cases are presented in this section, which include (i) alignment with load (MTC-one tape), (ii) misalignment with load (MTC-one tape), and (iii) drone flight time and battery life results.

A. FIRST EXPERIMENT: ALIGNMENT WITH LOAD (MTC-ONE TAPE)

The FSC was tested with the second coil, which was previously shown in Figure 1(d). The second coil consists of one tap with 60 turns. The experiment was implemented for an alignment system under a load condition (i.e., drone battery). This number of turns was selected based on the results of the first and second experiments, wherein a tradeoff was achieved between the coil weight and the transfer performance (transfer power and efficiency). Figure 7(a), 7(b), 7(c), and 7(d) show the AC output voltage of the MTC at different distances. Figure 7(a), 7(b), and 7(c) illustrate a pure sine wave at distances of 0, 1, and 4 cm, respectively. Figure 7(d) shows the sine wave with its distorted spectrum and the shape of the signal close to a square wave, which was due to the increased distance with the presence of a load. However, the amplitude of the signal was attenuated when the distance was increased.

The relationships between the transfer distance, the DC output power (right y-axis), and the transfer efficiency (left y-axis) are shown in Figure 8. The figure shows the performance of the MTC under the tested distance of 0–24 cm with a load. The figure shows that the DC output power decreased with distance. The DC output power and efficiency were 20.46 W and 85.25%, respectively, at 0 cm. The DC output power and efficiency decreased to 15.4 W and 64.16%, respectively, at 1 cm. However, they rapidly decreased to 4.2 W and 17.5% at 4 cm. Furthermore, the DC output power and efficiency were gradually decreased with distances beyond 4 cm.

B. SECOND EXPERIMENT: MISALIGNMENT WITH LOAD (MTC-ONE TAPE)

The FSC was tested with the MTC with 60 coil turns for several misalignment situations under a load condition (i.e., drone battery) to explore the transfer DC power and efficiency. The experiment was carried out for a lateral misalignment between the FSC and the MTC at four distances of 1, 5, 10, and 20 cm. The transfer DC power and transfer efficiency were recorded for these cases, as shown in Figure 9(a) and 9(b), respectively. For each lateral misalignment, the vertical distances between the transmitter coil (on the pad of the base station) and the receiver coil (mounted on the drone) were investigated in the range of 0–24 cm, as shown in Figure 9.

The maximum transfer DC power (17.1 W) and efficiency (71.25%) were recorded at 1 cm lateral misalignment and at 0 cm vertical distance. Transfer DC output powers of 9.9, 4.316, and 2.451 W were noted at 5, 10, and 20 cm lateral misalignments, respectively, for 0 cm vertical distance. The transfer power decreased with distance for all lateral misalignments and vertical distances, as shown in Figure 9(a).

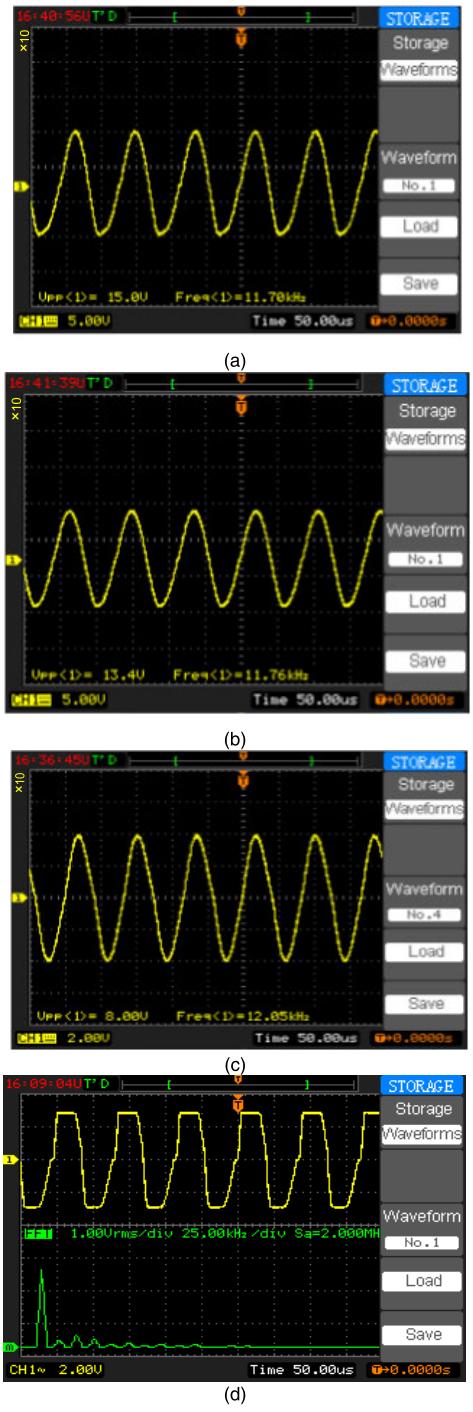

FIGURE 7. Output waveforms of MTC with load at (a) 0 cm, (b) 1 cm, (c) 4 cm, and (d) 6 cm.

Transfer efficiencies of 41%, 17.98%, and 10.21% were recorded at 5, 10, and 20 cm lateral misalignment, respectively, for 0 cm vertical distance. The transfer efficiency decreased with distance for all lateral misalignments and vertical distances, as shown in Figure 9(b).

C. DRONE FLIGHT TIME AND BATTERY LIFE RESULTS

The drone flight time and battery life can be estimated based on Equations (6–9) presented in Section IV, A, as shown

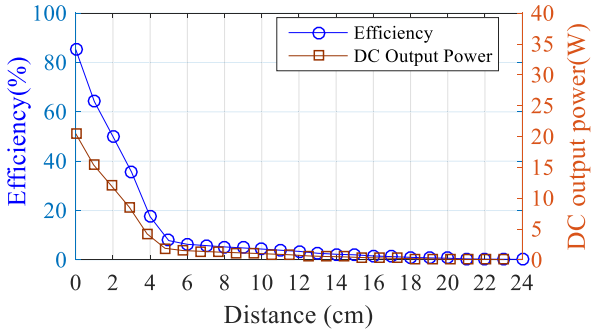

FIGURE 8. Performance of WPT (DC output power and efficiency) for MTC with 60 turns.

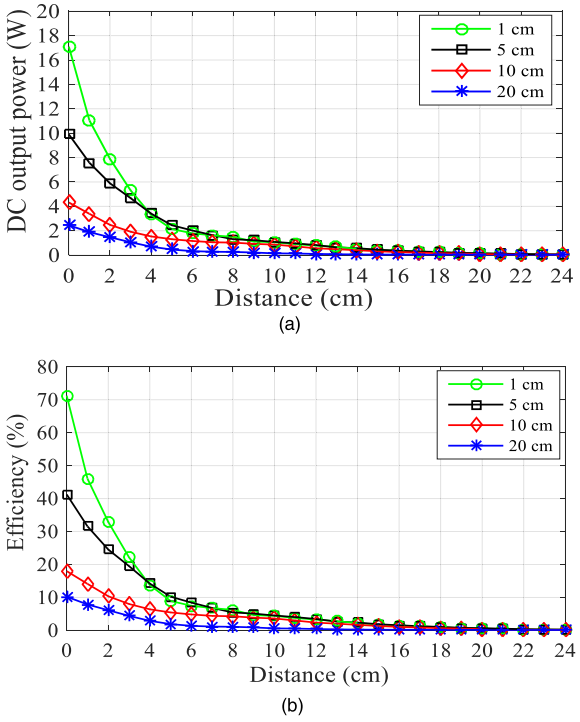

FIGURE 9. Performance of MTC with 60 coil turns in lateral misalignment; (a) DC output power and (b) transfer efficiency.

TABLE 4. Calculation of drone flight time.

Parameter	Value
W_T (kg)	1.892
P (W/kg)	120
V (V)	22.2
A_d (A), based on Eq. (7)	10.216
C_b (Ah)	5.5
D_b	80%
F_t (h), based on Eq. (6)	0.43 h (25.84 min)

in Table 4. Table 4 shows that the drone can fly for 25.84 min using a 5.5 Ah/22.2 Li-Po battery. This period can be extended when the battery capacity increases to 8 Ah or over. However, in this case, the drone payload will be increased. Therefore, a tradeoff between flight time and drone payload is necessary. Table 5 presents the measurements of the drone battery life with and without the sleep/active strategy.

TABLE 5. Comparison between the proposed MTC method at alignment conditions and previous studies.

Ref	Types of drone	Technique	Payload (g)	Flight time (minute)	Frequency (kHz)	Distance (cm)	Output power (W)	Transfer efficiency (%)
[30]/2012	Qud. AscTec Hummingbird	MRC	76	15–20	190–210	4	12.5 @ 4 cm	40
[12]/2017	Parrot bebop drone 1	CC	N/A	12	6,780	zero	12	50
[11]/2017	Qud. AR. drone 2.0	IC	N/A	12	N/A	zero	10	75
MTC (this work)	Qud. DJI X525	MRC	290	25.84	12	zero	20.46	85.25
MRC: Magnetic resonator coupling; IC: Inductive coupling; CC: Capacitive coupling; Qud.: Quadcopter								

TABLE 6. Near field comparison with other previous works.

Ref	Number of turns (T)		Type of shape coil	Transfer power (W)	Transfer distance (mm)	Transfer efficiency (%)	Frequency (kHz)
	Tx	Rx					
[40]/2019 (based-CWC)	5 and 10	10	circular	64.87	6	57.94	364.44
[41]/2018 (based-CWC)	2	1	circular	13	75	60	13560
[42]/2017 (based-CWC)	5	5	square	2.8	22.5	41.7	13560
[43]/2016 (based-CWC)	9	9	circular	3.1	0.6	48.2-51.2	110-210
[44]/2015 (based-CWC)	14	14	square and circular	0.1	10.4	30	6780
[45]/2015 (based-CWC)	9	9	circular	4.5	N/A	65	97.56
This work (based-CWC)	MTC 150	FSC 60	circular	20.46 @ 0 15.4 @ 100 12 @ 200	0, 100, and 200	85.25 @ 0 64.16 @ 100 50 @ 200	12
CWC: copper wire coil							

In a traditional operation (i.e., without sleep/active strategy), the battery life lasts 25.84 min. However, it can be extended to 851 min based on the sleep/active strategy. In the strategy, we assumed one drone mission every 4 h to collect the climate conditions of the farm field. The drone mission duration of approximately 5 min was required in the farm field to collect the sensor information, and the resting time was 235 min. This means that the drone consumes 2.127% (5/235) of the battery during each mission.

As a result, 96.9% of the drone battery's power savings can be achieved based on Equation (10). However, this percentage may be increased or decreased based on the duration of the drone's mission to collect data from the sensor nodes in the farm field. The time required to charge the battery fully, B_T, can be expressed in Equation (11). Hence, approximately 15 h was required to charge the adopted Li-Po battery fully with a 5.5 Ah capacity when the charging rate current, A_c, which equaled 370 mA, was considered at 0 cm between the drone's transmitter and receiving coils.

$$B_T = C_b / A_c \tag{11}$$

The battery life was prolonged to 851 min (14 h) based on sleep/active strategy. This value enabled the drone to make approximately 170 missions, i.e. 851 min/5 min of estimated value until the battery needed to be recharged. In other words, the battery life enabled the drone to conduct missions for 28 days (170 mission/6 missions per day) without needing to be recharged. For each experiment, the drone was on the landing pad for 235 min (3 h and 55 min), wherein the battery of the drone was charged. Therefore, the battery of the drone can be charged for 658 h in 28 days (235 landing time × 6 times charging per day × 28 days/60), wherein 15 h was enough to charge the battery fully. This value (i.e., 658 h) was 43 times the time required to charge the battery of the drone fully.

The tradeoff between weight and power transfer efficiency is critical for the drone payload. The weight reduction comes with the expense of reduction in power transfer efficiency. Based on the payload capability, the considered drone can still carry the developed wireless charger circuit (secondary coil) which form 52.25% from the total payload (555g). Additionally, a drone that carry higher payload will benefit from higher power transfer efficiency. In this study, the transfer efficiency was tested with 71% in misalignment conditions and the transfer power was 17.1 W that is adequate to charge the battery of drone within 15 hours.

VI. RESULTS COMPARISON

Several articles on WPTs adopted to provide drones with energy were compared with our proposed WPT system. The comparison was achieved based on performance metrics, such as transfer efficiency, power, and distance, adopted WPT, type of drone, payload of drone, and drone flight time for alignment systems, as shown in Table 5. In addition, near-field WPT that is adopted in this work using FSC and MTC was compared with previous works as shown in Table 6. The previous methods were similar to our work in that they utilized copper wires in the coil design. The proposed FSC (transmitter) and MTC (receiver) methods are closely related to the models of previous studies in terms of transfer efficiency and DC output power.

VII. CONCLUSION

Two experiments on proposed autonomous WPT systems were conducted in this study to select the optimum solution

that can charge the battery of the drone assigned to collect the climate conditions related to the agriculture of the farm field. Based on these experiments, the FSC coil with 150 coil turns in the transmitter circuit and the MTC comprised of 60 coil turns in the receiver (i.e., drone) were selected to accomplish the maximum transfer power and efficiency from the source coil to the drone.

The alignment and misalignment between the transmitter and receiver coils were investigated in terms of transfer power and efficiency. The battery of the drone was efficiently charged based on the proposed WPT system, and the drone can be collected from the climate conditions of the farm field during the missions.

The drone flight time was estimated based on the adopted battery capacity and the payload of the drone, which mainly depended on the coil weight. Compared with the conventional operation (i.e., 25.84 min), the battery of the drone was prolonged to 851 min based on the sleep/active strategy. This means the battery life of the drone was 32 times greater than the battery life in traditional operations. However, the power consumption may be increased when the active time is increased and vice versa. The power consumption of the mobile router node, which was carried by a drone, was improved based on the solar cell. In addition, future experiments can incorporate the use of wireless Internet of Things (IoT) technologies, such as LoRA, SigFox, and embed relevant agriculture sensors for monitoring farm field climate conditions, such as wind speed and direction, soil temperature, CO_2 concentrations, light intensity, barometric pressure, and rainfall.

Acknowledgment

The authors would like to thank Al-Rafidain University College for their generosity in financial assistance.

REFERENCES

[1] B. S. Faiçal, F. G. Costa, G. Pessin, J. Ueyama, H. Freitas, A. Colombo, P. H. Fini, L. Villas, P. S. Osório, P. A. Vargas, and T. Braun, "The use of unmanned aerial vehicles and wireless sensor networks for spraying pesticides," *J. Syst. Archit.*, vol. 60, no. 4, pp. 393–404, Apr. 2014.

[2] M. Bacco, E. Ferro, and A. Gotta, "UAVs in WSNs for agricultural applications: An analysis of the two-ray radio propagation model," in *Proc. IEEE SENSORS*, Nov. 2014, pp. 130–133.

[3] J. Valente, D. Sanz, A. Barrientos, J. del Cerro, Á. Ribeiro, and C. Rossi, "An air-ground wireless sensor network for crop monitoring," *Sensors*, vol. 11, no. 6, pp. 6088–6108, Jun. 2011.

[4] P. Sarunic and R. Evans, "Hierarchical model predictive control of UAVs performing multitarget-multisensor tracking," *IEEE Trans. Aerosp. Electron. Syst.*, vol. 50, no. 3, pp. 2253–2268, Jul. 2014.

[5] B. Lee, S. Kwon, P. Park, and K. Kim, "Active power management system for an unmanned aerial vehicle powered by solar cells, a fuel cell, and batteries," *IEEE Trans. Aerosp. Electron. Syst.*, vol. 50, no. 4, pp. 3167–3177, Oct. 2014.

[6] J. D. Renwick, L. J. Klein, and H. F. Hamann, "Drone-based reconstruction for 3D geospatial data processing," in *Proc. IEEE 3rd World Forum Internet Things (WF-IoT)*, Dec. 2016, pp. 729–734.

[7] M. Lu, M. Bagheri, A. P. James, and T. Phung, "Wireless charging techniques for UAVs: A review, reconceptualization, and extension," *IEEE Access*, vol. 6, pp. 29865–29884, 2018.

[8] D. Lee, J. Zhou, and W. T. Lin, "Autonomous battery swapping system for quadcopter," in *Proc. Int. Conf. Unmanned Aircraft Syst. (ICUAS)*, 2015, pp. 118–124.

[9] M. Dallachiesa, A. Puiatti, S. Knorr, and L. Puiatti, "Charging apparatus and method for electrically charging energy storage devices," U.S. Patent 20 160 336 772 A1, Nov. 17, 2016.

[10] S. Aldhaher, P. D. Mitcheson, J. M. Arteaga, G. Kkelis, and D. C. Yates, "Light-weight wireless power transfer for mid-air charging of drones," in *Proc. Eur. Conf. Antennas Propag. (EUCAP)*, Mar. 2017, pp. 336–340.

[11] A. B. Junaid, A. Konoiko, Y. Zweiri, M. N. Sahinkaya, and L. Seneviratne, "Autonomous wireless self-charging for multi-rotor unmanned aerial vehicles," *Energies*, vol. 10, no. 6, p. 803, Jun. 2017.

[12] T. M. Mostafa, A. Muharam, and R. Hattori, "Wireless battery charging system for drones via capacitive power transfer," in *Proc. IEEE PELS Workshop Emerg. Technol., Wireless Power Transf. (WoW)*, May 2017, pp. 1–6.

[13] T. Campi, S. Cruciani, M. Feliziani, and F. Maradei, "High efficiency and lightweight wireless charging system for drone batteries," in *Proc. AEIT Int. Annu. Conf.*, Sep. 2017, pp. 1–6.

[14] H. Wang and J. Shen, "Analysis of the characteristics of solar cell array based on MATLAB/simulink in solar unmanned aerial vehicle," *IEEE Access*, vol. 6, pp. 21195–21201, 2018.

[15] H. Shakhatreh, A. Sawalmeh, A. Al-Fuqaha, Z. Dou, E. Almaita, I. Khalil, N. S. Othman, A. Khreishah, and M. Guizani, "Unmanned aerial vehicles: A survey on civil applications and key research challenges," Apr. 2018, *arXiv:1805.00881*. [Online]. Available: https://arxiv.org/abs/1805.00881

[16] M. Hassanalian and A. Abdelkefi, "Classifications, applications, and design challenges of drones: A review," *Progr. Aerosp. Sci.*, vol. 91, pp. 99–131, May 2017.

[17] B. Kranjec, S. Sladic, W. Giernacki, and N. Bulic, "PV system design and flight efficiency considerations for fixed-wing radio-controlled aircraft—A case study," *Energies*, vol. 11, no. 10, p. 2648, 2018.

[18] M. H. Shaheed, A. Abidali, J. Ahmed, S. Ahmed, I. Burba, P. J. Fani, G. Kwofie, K. Wojewoda, and A. Munjiza, "Flying by the sun only: The solarcopter prototype," *Aerosp. Sci. Technol.*, vol. 45, pp. 209–214, Sep. 2015.

[19] V. Dobrokhodov, K. Jones, C. Dillard, and I. Kaminer, "Aqua-Quad-solar powered, long endurance, hybrid mobile vehicle for persistent surface and underwater reconnaissance, Part II-onboard intelligence," in *Proc. OCEANS MTS/IEEE Monterey*, Sep. 2016, pp. 1–9.

[20] N. Kingry, L. Towers, Y.-C. Liu, Y. Zu, Y. Wang, B. Staheli, Y. Katagiri, S. Cook, and R. Dai, "Design, modeling and control of a solar-powered quadcopter," in *Proc. IEEE Int. Conf. Robot. Automat. (ICRA)*, May 2018, pp. 1251–1258.

[21] L. Blain. *In-Flight Charging Gives Drones Unlimited Autonomous Range*. Accessed: Mar. 20, 2018. [Online]. Available: https://newatlas.com/in-air-drone-charging-unlimited-range/56363

[22] T. Campi, F. Dionisi, S. Cruciani, V. De Santis, M. Feliziani, and F. Maradei, "Magnetic field levels in drones equipped with wireless power transfer technology," in *Proc. Asia–Pacific Int. Symp. Electromagn. Compat. (APEMC)*, May 2016, pp. 544–547.

[23] C. H. Choi, H. J. Jang, S. G. Lim, H. C. Lim, S. H. Cho, and I. Gaponov, "Automatic wireless drone charging station creating essential environment for continuous drone operation," in *Proc. Int. Conf. Control, Automat. Inf. Sci. (ICCAIS)*, Oct. 2016, pp. 132–136.

[24] X. He, J. Bito, and M. M. Tentzeris, "A drone-based wireless power transfer anc communications platform," in *Proc. IEEE Wireless Power Transf. Conf. (WPTC)*, May 2017, pp. 1–4.

[25] D. Zorbas and C. Douligeris, "Computing optimal drone positions to wirelessly recharge IoT devices," in *Proc. IEEE Conf. Comput. Commun. Workshops (INFOCOM WKSHPS)*, Apr. 2018, pp. 628–633.

[26] C. Song, H. Kim, Y. Kim, D. Kim, S. Jeong, Y. Cho, S. Lee, S. Ahn, and J. Kim, "EMI reduction methods in wireless power transfer system for drone electrical charger using tightly coupled three-phase resonant magnetic field," *IEEE Trans. Ind. Electron.*, vol. 65, no. 9, pp. 6839–6849, Sep. 2018.

[27] A. M. Jawad, R. Nordin, S. K. Gharghan, H. M. Jawad, M. Ismail, and M. J. Abu-AlShaeer, "Single-tube and multi-turn coil near-field wireless power transfer for low-power home appliances," *Energies*, vol. 11, no. 8, p. 1969, 2018.

[28] T. Campi, S. Cruciani, and M. Feliziani, "Wireless power transfer technology applied to an autonomous electric UAV with a small secondary coil," *Energies*, vol. 11, no. 2, pp. 352-1–352-15, Feb. 2018.

[29] J. Zhou, B. Zhang, W. Xiao, D. Qiu, and Y. Chen, "Nonlinear parity-time-symmetric model for constant efficiency wireless power transfer: Application to a drone-in-flight wireless charging platform," *IEEE Trans. Ind. Electron.*, vol. 66, no. 5, pp. 4097–4107, May 2019.

[30] B. Griffin and C. Detweiler, "Resonant wireless power transfer to ground sensors from a UAV," in *Proc. IEEE Int. Conf. Robot. Automat. (ICRA)*, May 2012, pp. 2660–2665.
[31] C. Wang and Z. Ma, "Design of wireless power transfer device for UAV," in *Proc. IEEE Int. Conf. Robot. Automat. (ICRA)*, Aug. 2016, pp. 2449–2454.
[32] J. Polo, G. Hornero, C. Duijneveld, A. García, and O. Casas, "Design of a low-cost wireless sensor network with UAV mobile node for agricultural applications," *Comput. Electron. Agricult.*, vol. 119, pp. 19–32, Nov. 2015.
[33] A. Mittleider, B. Griffin, and C. Detweiler, "Experimental analysis of a uav-based wireless power transfer localization system," in *Proc. Experim. Robot., 14th Int. Symp. Experim. Robot.*, M. A. Hsieh, O. Khatib, and V. Kumar, Eds. Switzerland, 2016, pp. 357–371.
[34] Y. Gao, K. B. Farley, and Z. T. H. Tse, "A uniform voltage gain control for alignment robustness in wireless EV charging," *Energies*, vol. 8, no. 8, pp. 8355–8370, 2015.
[35] J. M. Arteaga, S. Aldhaher, G. Kkelis, D. C. Yates, and P. D. Mitcheson, "Multi-MHz IPT Systems for Variable Coupling," *IEEE Trans. Power Electron.*, vol. 33, no. 9, pp. 7744–7758, Sep. 2018.
[36] M. Rozman, M. Fernando, B. Adebisi, K. M. Rabie, T. Collins, R. Kharel, and A. Ikpehai, "A new technique for reducing size of a wpt system using two-loop strongly-resonant inductors," *Energies*, vol. 10, no. 10, p. 1614, Oct. 2017.
[37] G. Monti, A. Costanzo, F. Mastri, and M. Mongiardo, "Optimal design of a wireless power transfer link using parallel and series resonators," *Wireless Power Transf.*, vol. 3, pp. 105–116, Sep. 2016.
[38] T. Campi, S. Cruciani, V. De Santis, and M. Feliziani, "EMF safety and thermal aspects in a pacemaker equipped with a wireless power transfer system working at low frequency," *IEEE Trans. Microw. Theory Techn.*, vol. 64, no. 2, pp. 375–382, Feb. 2016.
[39] A. Rittiplang and W. Pijitrojana, "A low frequency wireless power transfer using parallel resonance under impedance matching," *Appl. Mech. Mater.*, vol. 781, pp. 410–413, Aug. 2015.
[40] C. Yang, Y. He, H. Qu, J. Wu, Z. Hou, Z. Lin, and C. Cai, "Analysis, design and implement of asymmetric coupled wireless power transfer systems for unmanned aerial vehicles," *AIP Adv.*, vol. 9, no. 2, 2019, Art. no. 025206.
[41] J. M. Arteaga, S. Aldhaher, G. Kkelis, C. Kwan, D. C. Yates, and P. D. Mitcheson, "Dynamic capabilities of multi-MHz inductive power transfer systems demonstrated with batteryless drones," *IEEE Trans. Power Electron.*, vol. 34, no. 6, pp. 5093–5104, Jun. 2018.
[42] J.-F. Chen, Z. Ding, Z. Hu, S. Wang, Y. Cheng, M. Liu, B. Wei, and S. Wang, "Metamaterial-based high-efficiency wireless power transfer system at 13.56 MHz for low power applications," *Prog. Electromagn. Res.*, vol. 72, pp. 17–30, 2017. doi: 10.2528/PIERB16071509.
[43] P. Worgan, J. Knibbe, M. Fraser, and D. M. Plasencia, "Powershake: Power transfer interactions for mobile devices," in *Proc. CHI Conf. Hum. Factors Comput. Syst.*, 2016, pp. 4734–4745.
[44] J. Kim, D.-H. Kim, J. Choi, K.-H. Kim, and Y.-J. Park, "Free-positioning wireless charging system for small electronic devices using a bowl-shaped transmitting coil," *IEEE Trans. Microw. Theory Techn.*, vol. 63, no. 3, pp. 791–800, Mar. 2015.
[45] W. X. Zhong and S. Y. R. Hui, "Maximum energy efficiency tracking for wireless power transfer systems," *IEEE Trans. Power Electron.*, vol. 30, no. 7, pp. 4025–4034, Jul. 2015.

AQEEL MAHMOOD JAWAD received the B.Sc. degree in computer and communication engineering from the Al-Rafidain University College, Iraq, in 2009, and the M.Sc. degree in electrical engineering from Universiti Tenaga National (UNITEN), Malaysia, in 2014. He is currently pursuing the Ph.D. degree with the Department of Electrical, Electronics and Systems Engineering, Faculty of Engineering and Built Environments, Universiti Kebangsaan Malaysia. He is also a Lecturer with the Department of Computer and Communication Engineering, Al-Rafidain University College, Baghdad, Iraq, where he is the Head of the Communication Lab. His research interests include wireless communications, transmutation line and digital communication, satellite communications theory, energy-efficient wireless power transfer, WPT charging applications based on unmanned aerial vehicle (UAV) techniques, advanced mathematics, and wireless sensor networks applications.

HAIDER MAHMOOD JAWAD received the B.Sc. degree in computer and communication engineering from the Al-Rafidain University College, Iraq, in 2007, and the M.Sc. degree in electrical engineering from Universiti Tenaga Nasional (UNITEN), Malaysia, 2014. He is currently pursuing the Ph.D. degree with the Department of Electrical, Electronics and Systems Engineering, Faculty of Engineering and Built Environments, Universiti Kebangsaan Malaysia. He is also a Lecturer with the Department of Computer and Communication Engineering, Al-Rafidain University College, Baghdad, Iraq, where he is a Supervisor with the Electronic Engineering Lab. His research interests include wireless communications, advanced communication theory, digital communications, unmanned aerial vehicle (UAV) applications, and wireless sensor networks applications.

ROSDIADEE NORDIN received the B.Eng. degree from Universiti Kebangsaan Malaysia, in 2001, and the Ph.D. degree from the University of Bristol, U.K., in 2011. He is currently an Associate Professor with the Centre of Advanced Electronic and Communication Engineering, Universiti Kebangsaan Malaysia, majoring in subjects related to wireless networks and mobile communications. His research interests include wireless sensor networks, the wireless Internet of Things (IoT), channel modeling, resource allocation and next generation wireless communication techniques, such as massive-MIMO for fifth generation (5G) networks.

SADIK KAMEL GHARGHAN received the B.Sc. degree in electrical and electronics engineering and the M.Sc. degree in communication engineering from the University of Technology, Iraq, in 1990 and 2005, respectively, and the Ph.D. degree in communication engineering from Universiti Kebangsaan Malaysia (UKM), Malaysia, in 2016. He is currently an Assistant Professor with the Department of Medical Instrumentation Techniques Engineering, Electrical Engineering Technical College, Middle Technical University (MTU), Baghdad, Iraq. His research interests include energy-efficient wireless sensor networks, biomedical sensors, microcontroller applications, WSN localization based on artificial intelligence techniques and optimization algorithms, indoor and outdoor path loss modeling, harvesting technique, wireless power transfer, and jamming on direct sequence spread spectrums.

NOR FADZILAH ABDULLAH received the B.Sc. degree in electrical and electronics from Universiti Teknologi Malaysia (UTM), in 2001, the M.Sc. degree in communications engineering from The University of Manchester, U.K., in 2001, and the Ph.D. degree in electrical and electronic engineering from the University of Bristol, U.K., in 2012. She was with telecommunication companies, such as Ericsson (Malaysia) and Maxis Communications Berhad (Malaysia), from 2003 to 2008. She is currently a Senior Lecturer with Universiti Kebangsaan Malaysia (UKM). Her research interests include 5G, millimeter wave, vehicular networks, MIMO, space time coding, and fountain codes as well as channel propagation modeling and estimation.

MAHMOOD JAWAD ABU-ALSHAEER received the B.Sc. and M.Sc. degrees in statistical science and the Ph.D. degree from the University of Baghdad, Iraq, in 1977, 1981, and 1997, respectively. He is currently a Professor with the Department of Computer and Communication Engineering, Al-Rafidain University College, where he is also a Lecturer and the Head of the Communication Department. His research interests include statistics, operation research, sampling techniques, time series, forecasting techniques, and advanced mathematics engineering.